ISPACS
International Scientific
Publications and Consulting Services

Available online at www.ispacs.com/cna
Volume 2011, Year 2011 Article ID cna-00109, 20 pages
doi: 10.5899/2011/cna-00109
Research Article

Communications in Numerical Analysis

Heat and Mass Transfer from MHD Flow over a Moving Permeable Cylinder with Heat Generation or Absorption and Chemical Reaction

Ali J. Chamkha*

Manufacturing Engineering Department The Public Authority for Applied Education and Training Shuweikh 70654, Kuwait

Abstract

General boundary-layer equations governing steady, laminar, hydromagnetic flow and heat and mass transfer over a permeable cylinder moving with a linear velocity in the presence of heat generation/absorption, chemical reaction, suction/injection effects and uniform transverse magnetic field are developed. A similarity transformation is used to transform the governing partial differential equations into ordinary differential equations. The dimensionless self-similar equations are then solved numerically by using a standard fully implicit, iterative, tri-diagonal finite-difference method. Comparisons with previously published work on various special cases of the problem are performed and the results are found to be in excellent agreement. A parametric study of the physical parameters involved in the problem is conducted and a representative set of numerical results is illustrated graphically and in tabular form.

Keywords : Moving cylinder; similarity solutions; MHD; suction/injection; chemical reaction; heat generation/absorption.

1 Introduction

Considerable work has been done on boundary-layer flow and heat transfer in a quiescent fluid driven by stretched surfaces moving with a constant or variable velocity. This is due to many metallurgical and engineering applications such as hot rolling, metal and

*Email address: achamkha@yahoo.com

polymer sheet extrusion, drawing, annealing and tinning of copper wires, crystal growth, glass fiber production, paper production, and many others. The first to consider flow and heat transfer over a continuously moving surface with a uniform velocity was Sakiadis [34, 35]. In later studies, Erickson et al. [17], Tsuo et al. [41], Fox et al. [18], Chen and Strobel [13], and Jacobi [26] verified and extended the works of Sakiadis [34, 35]. It is worthy to mention that Jacobi [26] confirmed experimentally the flow field obtained by Sakiadis [34, 35] for a uniform motion of the stretched surface.

There has also been research dealing with the problem of a stretched surface moving with a linear velocity and various thermal boundary conditions (see, for instance, Crane [16], Gupta and Gupta [23], Vleggar [44], Soundalgekar and Murty [37], Grubka and Bobba [22], and Chen and Char [12]). Later on, many investigations studied the consequent flow and heat transfer characteristics that are brought about by the movement of a stretched permeable and impermeable, isothermal and non-isothermal surface with a power-law velocity variation. Examples of these works are Banks [6] who considered the case of impermeable wall, Ali [3, 4] who presented various extensions to Banks' problem, [6], in terms of flow and thermal boundary conditions. Mahapatra and Gupta [29] studied heat transfer in stagnation-point flow towards a stretching sheet. Pop et al. [32] investigated radiation effects on the flow near the stagnation point of a stretching sheet.

There has been renewed interest in studying hydromagnetic flow and heat transfer of continuously stretched surfaces in the presence of a transverse magnetic field. This is because hydromagnetic flow and heat transfer have become more important industrially. For example, many metallurgical processes such as drawing, annealing and tinning of copper wires involve cooling of continuous strips or filaments by drawing them through a quiescent fluid. Controlling the rate of cooling in these processes can affect the properties of the final product. This can be done by using an electrically-conducting fluid and applying a magnetic field. Another application of hydromagnetics to metallurgy lies in the purification of molten metals from non-metallic inclusions (Vajravelu and Hadjinicolaou [42]). Cobble [15] obtained similarity solutions for hydromagnetic flow over a semi-infinite plate with suction and injection at the wall. Soundalgekar and Murty [37] had considered the thermal problem of Cobble, [15]. Chandran et al. [11] made extensions to the above works and considered flow of an electrically-conducting fluid over a semi-infinite plate with suction and injection. Chakrabarti and Gupta [9] obtained a closed-form similarity solution for the problem of hydromagnetic flow of a linearly stretching surface in the presence of a constant transverse magnetic field. Chiam [14] extended the work of Chakrabarti and Gupta [9] to power-law velocity of the stretched surface. Recently, Sharma and Singh [36], reported on the effects of variable thermal conductivity and heat source/sink on MHD flow near a stagnation point on a linearly stretching sheet.

There have been some work dealing with flow and/or heat and mass transfer caused by a moving cylinder. Bourne and Elliston [8] studies heat transfer through the axially symmetric boundary layer on a moving circular fibre. Krani and Pecho [27] reported on the thermal laminar boundary layer on a continuous cylinder. Rotte and Beek [33] reported some models for the calculation of heat transfer coefficients to a moving continuous cylinder. Takhar et al. [40] investigated combined heat and mass transfer along a vertical moving cylinder with a free stream. Pantokratoras [31] considered laminar assisting mixed convection heat transfer from a vertical isothermal cylinder moving in water at low temperatures. Ganesan and Loganathan [19] studied radiation and mass transfer effects on flow of an incompressible viscous fluid past a moving vertical cylinder. Also,

Ganesan and Loganathan [20] analyzed heat and mass flux effects on a moving vertical cylinder with chemically reactive species diffusion. Later, Ganesan and Loganathan [21] investigated magnetic field effect on a moving vertical cylinder with constant heat flux. Abo-Eldahab and Salem [1] considered MHD flow and heat transfer of non-newtonian power-law fluid with diffusion and chemical reaction on a moving cylinder. Amkandi and Azzouzi [5] reported on a similarity solution of MHD boundary layer flow over a moving vertical cylinder. Ishak et al.[24, 25] studied magnetohydrodynamic and suction/blowing effects for flow and heat transfer due to a stretching cylinder.

In certain industrial problems dealing with chemical reactions and dissociating fluids, heat generation/absorption and chemical reaction effects become important (see Vajravelu and Nayfeh [43]). Moalem [30] considered temperature-dependent heat sources occurring in electrical heating. Abo-Eldahab and Salem [1] considered chemical reaction effects on flow on a moving cylinder. Other works dealing with heat generation effects can be found in the papers by Sparrow and Cess [39], Chamkha [10], Vajravelu and Hadjinicolaou [42] and Ganesan and Loganathan [20].

The present paper deals with steady, laminar, hydromagnetic flow and heat and mass transfer along a permeable linearly moving cylinder with heat generation/absorption, chemical reaction and suction/injection effects in the presence of uniform transverse magnetic field.

2 Mathematical Formulation

Consider steady, laminar, hydromagnetic, two-dimensional boundary-layer near stagnation-point flow and heat and mass transfer in an electrically-conducting fluid driven by a vertical isothermal permeable cylinder moving with a linear velocity with heat generation/absorption and chemical reaction effects. Fluid suction or injection is imposed at the boundary of the cylinder and a uniform transverse magnetic field is applied normal to the flow direction. The external or free stream velocity is assumed to vary linearly with the axial distance. The working fluid is assumed to be incompressible, viscous, heat generating or absorbing, electrically conducting and has constant properties. The magnetic Reynolds number is assumed to be small so that the induced magnetic field can be neglected. In addition, no external electric field is assumed to exist and the electric field due to the effect of charge polarization and the Hall effect of magnetohydrodynamics are neglected. The effects of viscous dissipation and Joule heating are also neglected. The basic equations for this investigation can be written as:

$$\frac{\partial(ru)}{\partial x} + \frac{\partial(rv)}{\partial r} = 0 \tag{2.1}$$

$$u\frac{\partial u}{\partial x} + v\frac{\partial u}{\partial r} = \frac{\nu}{r}\frac{\partial}{\partial r}(r\frac{\partial u}{\partial r}) + u_e(x)\frac{\mathrm{d}u_e(x)}{\mathrm{d}x} - \frac{\sigma B^2}{\rho}[u_e(x) - u] \tag{2.2}$$

$$u\frac{\partial T}{\partial x} + v\frac{\partial T}{\partial r} = \frac{\alpha}{r}\frac{\partial}{\partial r}(r\frac{\partial T}{\partial r}) + \frac{Q}{\rho c_p}(T - T_\infty) \tag{2.3}$$

$$u\frac{\partial c}{\partial x} + v\frac{\partial c}{\partial r} = \frac{D}{r}\frac{\partial}{\partial r}(r\frac{\partial c}{\partial r}) - r_c(c - c_\infty) \tag{2.4}$$

where x and r are the axial and the radial distances, respectively. u, v, T, c, T_∞ and c_∞ are the fluid x-component and r-component of velocity, temperature, concentration, ambient temperature and the ambient concentration, respectively. ρ, ν, c_p, α and D are the fluid density, kinematic viscosity, specific heat at constant pressure, thermal diffusivity, and the mass diffusion respectively. σ, B, Q and r_c are the electrical conductivity, magnetic induction, heat generation/absorption coefficient and the chemical reaction coefficient, respectively. Here $u_e(x)$ is the variable external or free stream velocity. It should be mentioned that positive values of Q mean heat generation (source) and negative values of Q indicate heat absorption (sink). Also, it is noticed that the heat generation or absorption term is assumed to be dependent on the difference between the boundary-layer temperature and that of the free stream. This has been employed previously by Vajravelu and Hadjinicolaou [42] and is appropriate for boundary-layer applications in which this difference is significant.

The boundary conditions for this problem are:

$$u(x,R) = u_w x,\ v(x,R) = -v_w,\ T(R,0) = T_w,\ c(R,0) = C_w \tag{2.5}$$

$$u(x,\infty) = u_e(x) = u_\infty x,\ T(x,\infty) = T_\infty,\ c(x,\infty) = c_\infty$$

where u_w is a constant and v_w, T_w and c_w are the suction (> 0) or injection (< 0) velocity, wall temperature and wall concentration, respectively.

It is convenient to employ the following similarity transformations:

$$\eta = \sqrt{\frac{u_w}{2\nu}}\Big(\frac{r^2 - R^2}{R}\Big),\ \psi = \sqrt{\frac{\nu u_w}{2}} Rx f(\eta),\ \theta(\eta) = \frac{T - T_\infty}{T_w - T_\infty}, \tag{2.6}$$

$$C(\eta) = \frac{c - c_\infty}{c_w - c_\infty},\ u = \frac{1}{r}\frac{\partial \psi}{\partial r},\ v = -\frac{1}{r}\frac{\partial \psi}{\partial x}$$

where η, $f'(\eta)$, $\theta(\eta)$ and $C(\eta)$ are the similarity variable, dimensionless velocity, dimensionless temperature and the dimensionless concentration, respectively. Here, a prime denotes ordinary differentiation with respect to η. It can easily be verified that the balance of mass given by Equation (2.1) is identically satisfied.

Substitution of Equations (2.6) into Equations (2.2) through (2.4) and rearranging yields:

$$(2K\eta + 2)f''' + (K + f)f'' - (f')^2 - Ha^2(f' - \lambda) + \lambda^2 = 0 \tag{2.7}$$

$$(2K\eta + 2)\theta'' + (K + Prf)\theta' + Pr\phi\theta = 0 \tag{2.8}$$

$$(2K\eta + 2)C'' + (K + Scf)C' - Sc\gamma C = 0 \tag{2.9}$$

where

$$K = \frac{1}{R}\sqrt{\frac{2\nu}{u_w}},\ Ha^2 = \frac{\sigma B_0^2}{\rho u_y},\ \lambda = \frac{u_\infty}{u_w}, \tag{2.10}$$

$$Pr = \frac{\nu}{\alpha},\ \phi = \frac{Q}{\rho c_p u_w}, Sc = \frac{\nu}{D},\ \gamma = \frac{r_c}{u_w}.$$

Here, K is the curvature parameter, Ha is the Hartmann number, λ is the ratio of the free stream to cylinder stretching velocity, Pr is the Prandtl number, ϕ is the dimensionless heat generation/absorption coefficient which indicates heat generation for positive values and heat absorption for negative values, Sc is the Schmidt number and γ is the dimensionless chemical reaction parameter.

The transformed dimensionless boundary conditions become:

$$f'(0) = 1,\ f(0) = f_0,\ \theta(0) = 1,\ C(0) = 1, \tag{2.11}$$

$$f'(\infty) = \lambda,\ \theta(\infty) = 0,\ C(\infty) = 0.$$

where $f_0 = v_w\sqrt{\frac{2}{\nu u_w}}$ is the dimensionless suction ($f_0 > 0$) or injection ($f_0 < 0$) velocity. It should be mentioned that if f_0, Ha and K are formally set to zero and replacing the number 2 in the diffusive terms of Equations (2.7) and (2.8) by the number 1, the equations reported by Sharma and Singh [36] will be recovered.

Of special interest and significance for this flow and heat and mass transfer situation are the skin-friction coefficient C_f, Nusselt number Nu and the Sherwood number Sh. These are defined, respectively, as follows:

$$C_f = \frac{-\frac{\partial u}{\partial r}(x, R)}{u_w} = -\frac{1}{2}Re_x^{1/2}f''(0) \tag{2.12}$$

$$Nu = \frac{-x\frac{\partial T}{\partial r}(x, R)}{T_w - T_\infty} = -\frac{1}{2}Re_x^{1/2}\theta'(x, 0)$$

$$Sh = \frac{-x\frac{\partial c}{\partial r}(x, R)}{c_w - c_\infty} = -\frac{1}{2}Re_x^{1/2}C'(x, 0)$$

where $Re = \frac{u_w x^2}{\nu}$ is the local Reynolds number.

3 Numerical Method and Validation

The heat and mass transfer problem for the linearly moving cylinder represented by Equations (2.7) through (2.11) are nonlinear and, therefore, must be solved numerically. The standard implicit finite-difference method discussed by Blottner [7] has proven to be adequate and gives accurate results for such equations. For this reason, it is employed in the present work and graphical and tabular results based on this method will be presented subsequently.

Equations (2.7) and (2.8) are discretized using three-point central difference formulae with F' replaced by another variable V. The η direction is divided into 196 nodal points and a variable step size is used to account for the sharp changes in the variables in the region close to the cylinder surface where viscous effects dominate. The initial step size used is $\Delta\eta_1 = 0.001$ and the growth factor $K = 1.055$ such that $\Delta\eta_n = K\Delta\eta_{n-1}$ (where the subscript n is the number of nodes minus one). This gives $\eta_{max} \approx 600$ which represents the edge of the boundary layer at infinity. The ordinary differential equations are then converted into linear algebraic equations that are solved by the Thomas algorithm discussed by Blottner [7]. Iteration is employed to deal with the nonlinear nature of the governing equations. The convergence criterion employed in this work was based on the relative difference between the current and the previous iterations. When this difference or error reached 10^{-5}, then the solution was assumed converged and the iteration process was terminated. It is possible to compare the results obtained by this numerical method with other previously published work for the near stagnation-point on a linearly stretching surface ($K = 0$) if we replace the number 2 appearing in the $f'''(\eta)$ and $\theta''(\eta)$ terms by the number 1 in Equations (2.7) and (2.8).

Table 1 shows a comparison between the numerical results of $f''(0)$ for the case of impermeable surface ($f_0 = 0$), $K = 0$, $Ha = 0$ and various values of λ reported by Mahapatra and Gupta [29], Pop et al. [32] and Sharma and Singh [36] and the numerical results obtained in the present work. It is evident from this table that these results are in excellent agreement.

Table 1
Comparison of $f''(0)$ for $f_0 = 0$, $Ha = 0$, $K = 0$ and various values of λ.

λ	Mahapatra and Gupta [29]	Pop et al. [32]	Sharma and Singh [36]	Present results
0.1	-0.9694	-0.9694	-0.969386	-0.9694286
0.2	-0.9181	-0.9181	-0.9181069	-0.9180468
0.5	-0.6673	-0.6673	-0.667263	-0.6670318
2.0	2.0175	2.0174	2.01749079	2.0182771
3.0	4.7293	4.7290	4.72922695	4.7308391

Table 2 presents a comparison between the numerical results of $f''(0)$ for $f_0 = 0$, $K = 0$ and various values of Ha and λ reported by Sharma and Singh [36] and the present numerical results. The comparison shows excellent agreement between the results.

Table 2
Comparison of $f''(0)$ for $f_0 = 0$, $K = 0$ and various values of Ha and λ with Sharma and Singh [36].

λ	Ha	Sharma and Singh [36]	Present results
0.1	0.1	-0.97350851	-0.9734556
0.2	0.1	-0.921466	-0.9213231
0.5	0.1	-0.669102	-0.6689756
2.0	0.1	2.01993243	2.0206652
3.0	0.1	4.73339915	4.7335115
0.1	0.5	-1.067898	-1.0679350
0.2	0.5	-1.00469	-1.0004000
0.5	0.5	-0.71189085	-0.7117829
2.0	0.5	2.07771118	2.0783232
3.0	0.5	4.8325013	4.8330012
0.1	1.0	-1.321111	-1.3211361
0.2	1.0	-1.2156222	-1.2156172
0.5	1.0	-0.83212508	-0.8318299
2.0	1.0	2.2408579	2.2499462
3.0	1.0	5.13030441	5.1319281

Table 3 reports a comparison of $-\theta'(0)$ for $f_0 = 0$, $Ha = 0$, $K = 0$, $Pr = 0.05$, $\phi = 0$ and various values of λ reported by Mahapatra and Gupta [29], Pop et al. [32] and Sharma and Singh [36] and the present numerical results. It is clear from these tables that the present predicted results for $-\theta'(0)$ agree well with those reported by previous investigators.

Table 3
Comparison of $-\theta'(0)$ for $f_0 = 0$, $Ha = 0$, $K = 0$, $Pr = 0.05$, $\phi = 0$ and various values of λ.

λ	Mahapatra and Gupta [29]	Pop et al. [32]	Sharma and Singh [36]	Present results
0.1	0.081	0.081	0.081245	0.0753756
0.5	0.136	0.135	0.135571	0.1344137
2.0	0.241	0.241	0.241025	0.2423843

Finally, Table 4 gives a comparison of $-\theta'(0)$ for $f_0 = 0$, $K = 0$, $Pr = 0.023$, $\phi = 0$ and various values of Ha and λ with Sharma and Singh [36]. Favorable agreement between the results is apparent in this table. The excellent agreement shown between the present results in Tables 1-4 and the results of previous investigators lends confidence to the accuracy of the numerical procedure.

Table 4
Comparison of $-\theta'(0)$ for $f_0 = 0$, $K = 0$, $Pr = 0.023$, $\phi = 0$ and various values of Ha and λ with Sharma and Singh [36].

λ	Ha	Sharma and Singh [36]	Present results
0.1	0	0.049828	0.05012805
0.5	0	0.090049	0.09036328
2.0	0	0.165693	0.16604421
0.1	0.5	0.048889	0.04919378
0.5	0.5	0.089842	0.09017963
2.0	0.5	0.165796	0.16618262

4 Results and Discussion

Many numerical results were obtained throughout the course of this work. A representative set of these results is shown graphically in Figures 1 through 13 to illustrate special features for the hydrodynamic, thermal and solutal characteristics of the problem.

Figure 1 displays representative velocity profiles for various values of the velocity ratio λ. Increasing the value of λ means that free stream velocity increases in comparison to cylinder stretching velocity. This results in increased pressure and straining motion near stagnation point and hence increased velocity and thinning of the boundary layer takes place. It is important to note that for $\lambda = 1$ there is no formation of boundary layer because the cylinder velocity is equal to the free stream velocity. For values of $\lambda < 1$, the velocity profile shows a decreasing trend with η while for $\lambda > 1$, the velocity profile increases with η.

Figures 2 and 3 show the effects of the curvature parameter K on the velocity profiles for two different values of λ ($\lambda = 0.5$ and $\lambda = 1.5$), respectively. It is seen that the velocity increases as K increases for $\lambda = 0.5$ while it decreases with increasing values of K for $\lambda = 1.5$. However, the boundary layer thickness increases as K increases for both $\lambda = 0.5$

and $\lambda = 1.5$.

Figure 4 presents typical profiles for velocity for various values of the magnetic Hartmann number Ha for two different values of λ ($\lambda = 0.5$ and $\lambda = 1.5$). When $\lambda < 1$, application of a transverse magnetic field normal to the flow direction gives rise to a resistive force called the Lorentz force. This force has the effect of slowing down the motion of the fluid along the stretched cylinder. In addition, increasing the strength of the magnetic field further produces more reductions in the fluid velocity and in the boundary layer thickness. On the other hand, when $\lambda > 1$, the exact opposite effect is predicted. These characteristics are clearly shown in Figure 4.

Figure 5 displays the effects of the suction/injection parameter f_0 on the velocity profiles for two different values of λ ($\lambda = 0.5$ and $\lambda = 1.5$). As expected, for $\lambda < 1$, imposition of fluid suction ($f_0 > 0$) at the cylinder boundary reduces both the hydrodynamic boundary layers close to the wall and, therefore, the fluid velocity. On the other hand, injection ($f_0 < 0$) of fluid at the cylinder surface produces the opposite effect, namely increased hydrodynamic boundary layer and enhanced velocity field. The exact opposite behaviors is predicted for $\lambda > 1$. These behaviors are clearly illustrated by the decreases (increases) in the velocity profiles for $\lambda < 1$ ($\lambda > 1$) as the suction/injection parameter f_0 increases as shown in Figure 5.

Figures 6 and 7 depict the influence of the heat generation/absorption coefficient ϕ on the temperature profiles for $\lambda = 0.5$ and $\lambda = 1.5$, respectively. As expected, increases in the value of the heat generation/absorption coefficient ϕ cause the fluid temperature to increase. It should be noted that for large heat generation effects ($\phi = 0.4$ for $\lambda = 0.5$ and $\phi = 1.0$ for $\lambda = 1.5$) a distinctive peak in the temperature profile occurs in the region close to the cylinder surface. This is in contrast with the cases of smaller heat generation effects ($\phi < 0.3$ for $\lambda = 0.5$ and $\phi < 0.8$ for $\lambda = 1.5$) in which the maximum temperature occurs at the cylinder boundary. In addition, the thermal boundary layer thickness increases as ϕ increases. Furthermore, it is predicted that the effects of ϕ on the temperature profiles for $\lambda = 0.5$ are much more significant than those for $\lambda = 1.5$. These facts are clearly shown in Figures 6 and 7.

Figures 8 and 9 elucidate the effects of the chemical reaction parameter γ on the concentration profiles for $\lambda = 0.5$ and $\lambda = 1.5$, respectively. Increasing the value of γ has the tendency to decrease the solute concentration and its boundary layer. This is true for both $\lambda = 0.5$ and $\lambda = 1.5$. It is also observed from these two figures that the effects of γ on the concentration profiles are more pronounced for $\lambda = 0.5$ than those for $\lambda = 1.5$.

Figures 10 and 11 present the effects of the curvature parameter K on the temperature and concentration profiles for two different values of λ ($\lambda = 0.5$ and $\lambda = 1.5$), respectively. It is observed that significant increases occur in both the fluid temperature and solutal concentration as K increases. This is accompanied by significant increases in the thermal and concentrational boundary layer thicknesses as K increases for both $\lambda = 0.5$ and $\lambda = 1.5$. Also, increasing the value of λ is predicted to cause decreases in both the temperature and concentration profiles and their boundary layers.

Figures 12 and 13 illustrate the effects of the suction/injection parameter f_0 on the temperature and concentration profiles for two different values of λ ($\lambda = 0.5$ and $\lambda = 1.5$), respectively. As mentioned before, imposition of fluid suction ($f_0 > 0$) at the cylinder boundary reduces both the hydrodynamic, thermal and concentrational boundary layers close to the cylinder surface and, therefore, all of the fluid velocity, temperature and concentration. On the other hand, injection ($f_0 < 0$) of fluid at the cylinder surface pro-

duces the opposite effect, namely increased hydrodynamic, thermal and concentrational boundary layers and enhanced velocity, temperature and concentration fields. However, the increase or decrease in the various boundary layers is relative as it is dependent on the parametric values used to produce these figures. Again, the temperature and concentration profiles are higher for $\lambda = 0.5$ than those for $\lambda = 1.5$.

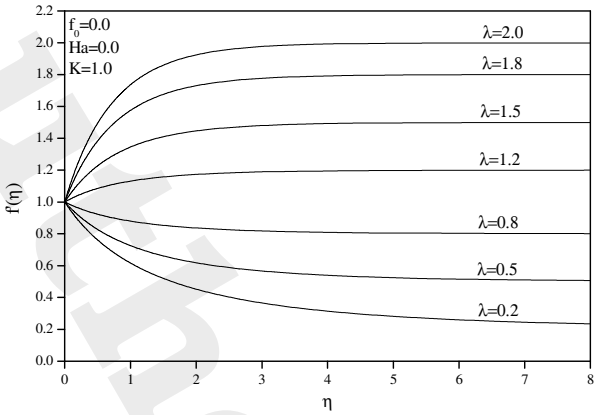

Figure 1. Effects of λ on velocity profiles

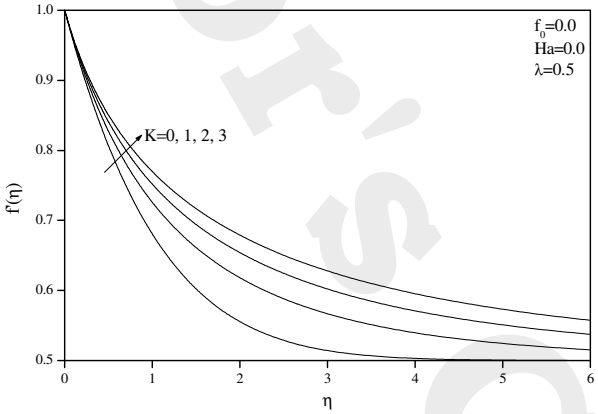

Figure 2. Effects of K on velocity profiles for λ=0.5

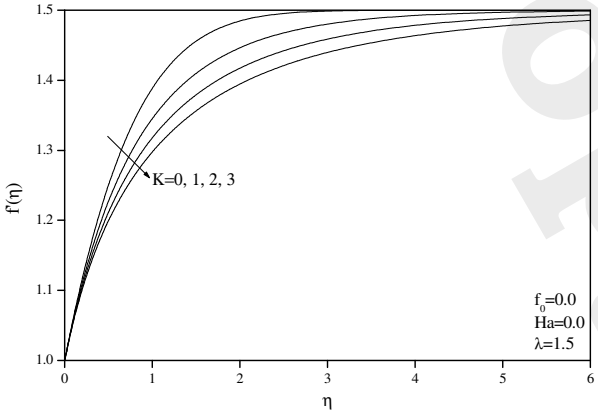

Figure 3. Effects of K on velocity profiles for λ=1.5

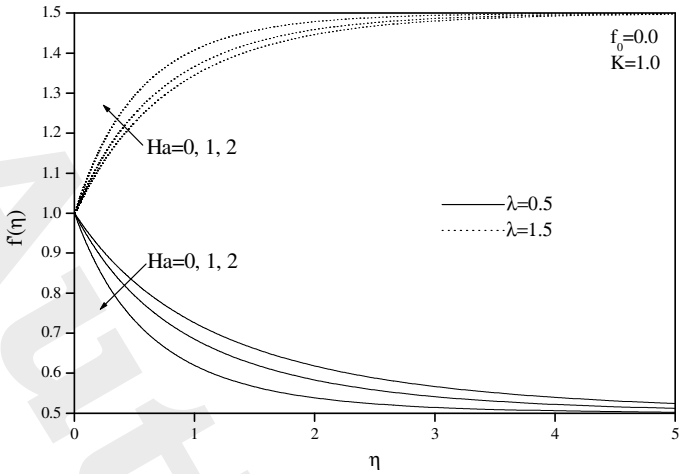

Figure 4. Effects of Ha on velocity profiles for λ=0.5 and λ=1.5

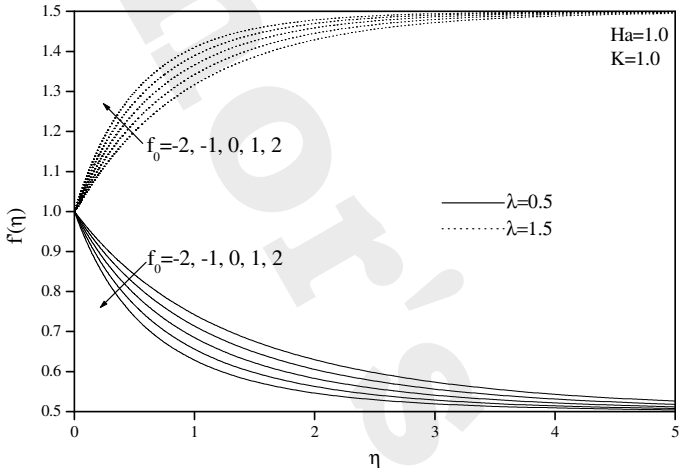

Figure 5. Effects of f_0 on velocity profiles for λ=0.5 and λ=1.5

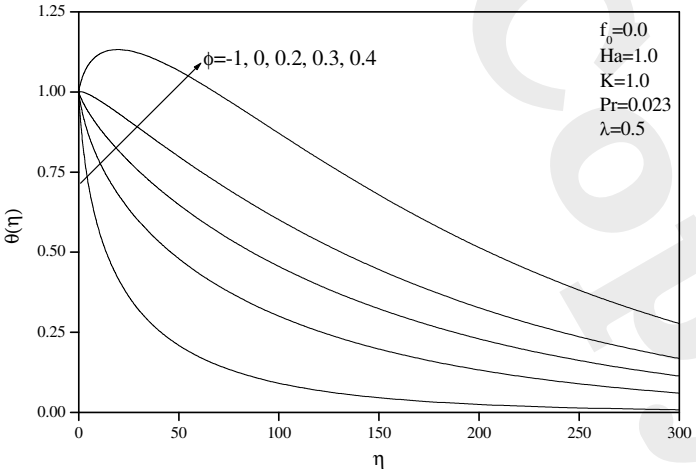

Figure 6. Effects of ϕ on temperature profiles for λ=0.5

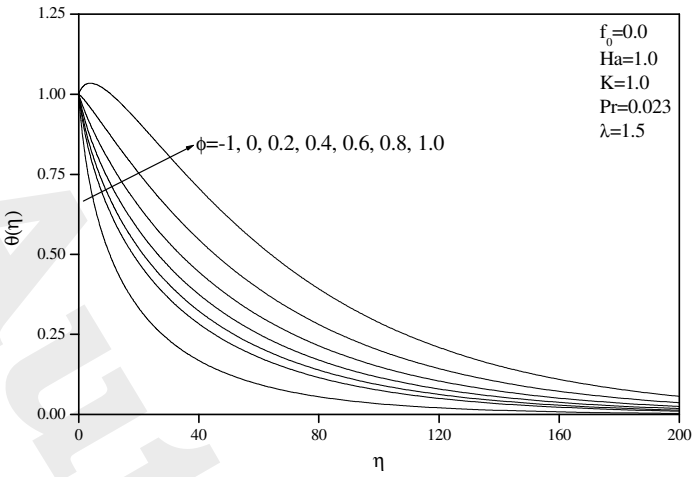

Figure 7. Effects of ϕ on temperature profiles for λ=1.5

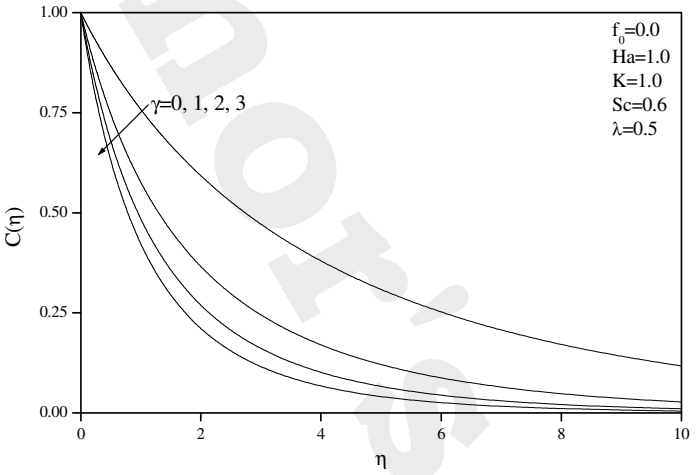

Figure 8. Effects of γ on concentration profiles for λ=0.5

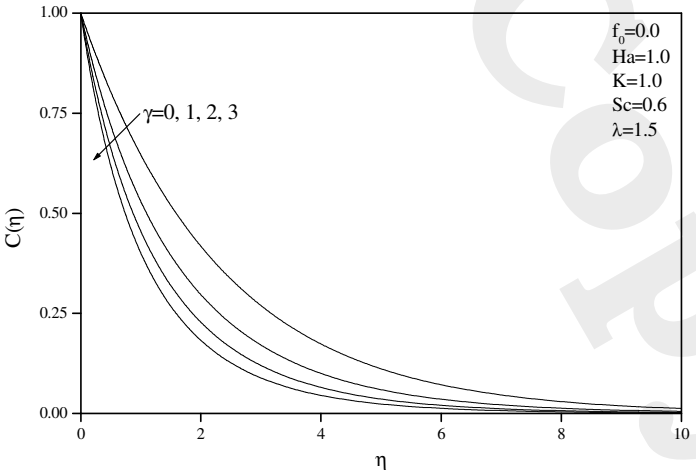

Figure 9. Effects of γ on concentration profiles for λ=1.5

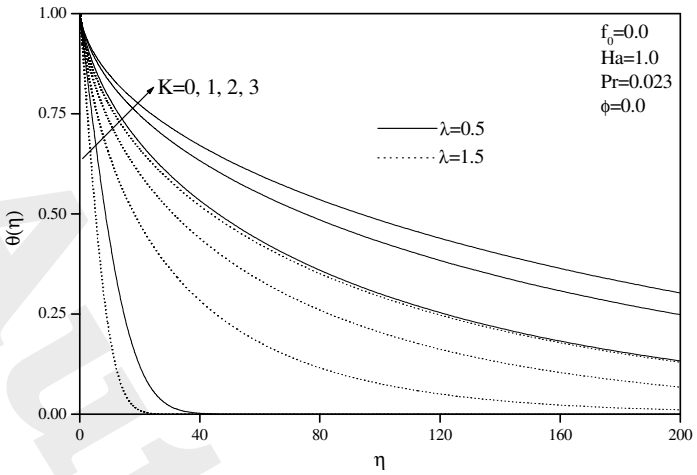

Figure 10. Effects of K on temperature profiles for λ=0.5 and λ=1.5

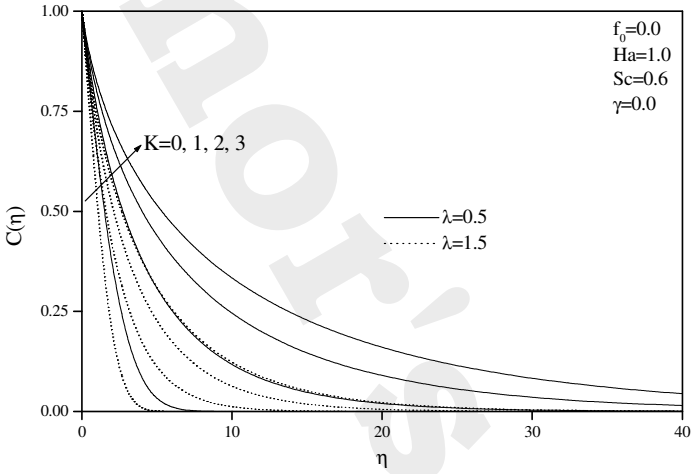

Figure 11. Effects of K on concentration profiles for λ=0.5 and λ=1.5

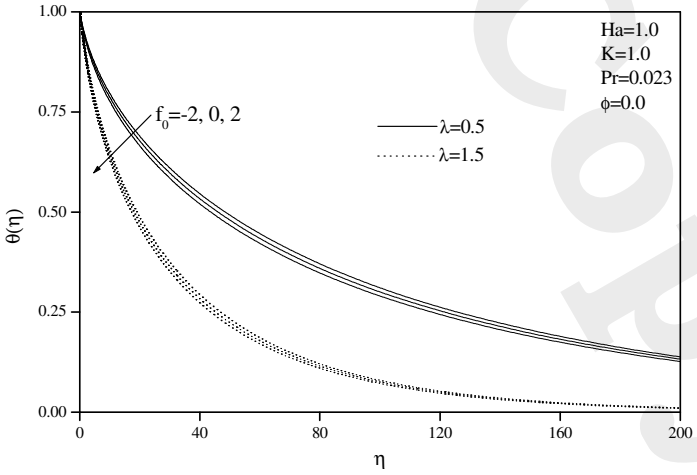

Figure 12. Effects of f_0 on temperature profiles for λ=0.5 and λ=1.5

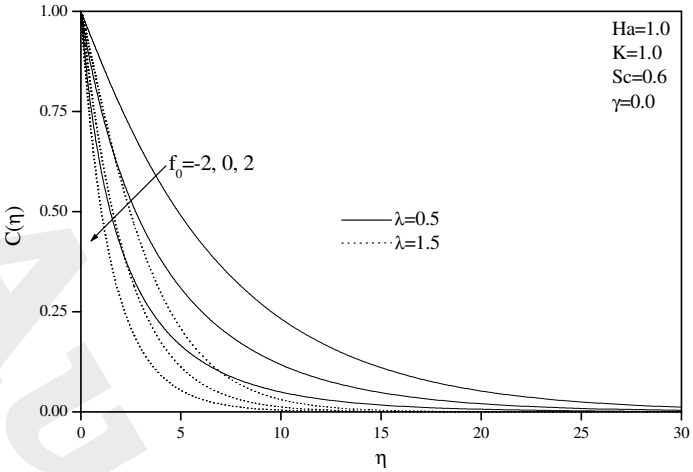

Figure 13. Effects of f_0 on concentration profiles for λ=0.5 and λ=1.5

Tables 5 through 8 illustrate the influence of the velocity ratio λ, curvature parameter K, Hartmann number Ha and the suction/injection coefficient f_0 on the values of $f''(0)$, respectively. It is evident from these tables that the value of $f''(0)$ are positive for $\lambda > 1$ and negative for $\lambda < 1$. Depending of the value of λ, the effects of the various parameters are different. When $\lambda < 1$, the value of $f''(0)$ increases as either of λ or K increases while it decreases as Ha or f_0 increases. On the other hand, when $\lambda > 1$, the value of $f''(0)$ increases as either of λ, Ha or f_0 increases while it decreases as K increases.

Table 5
Effects of λ on $f''(0)$ for $f_0 = 0$, $Ha = 0$ and $K = 1.0$.

λ	$f''(0)$
0.2	-0.6281865
0.5	-0.4607047
0.8	-0.2075934
1.2	0.2357507
1.5	0.6355050
1.8	1.085292
2.0	1.411189

Table 6
Effects of K on $f''(0)$ for $f_0 = 0$ and $Ha = 0$

λ	K	$f''(0)$
0.5	0.0	-0.4717014
0.5	1.0	-0.4607047
0.5	2.0	-0.4560649
0.5	3.0	-0.4531392
1.5	0.0	0.6437751
1.5	1.0	0.6355050
1.5	2.0	0.6307550
1.5	3.0	0.6278736

Table 7
Effects of Ha on $f''(0)$ for $f_0 = 0$ and $K = 1.0$.

λ	Ha	$f''(0)$
0.5	0.0	-0.4607047
0.5	1.0	-0.5811208
0.5	2.0	-0.8447003
1.5	0.0	0.6355050
1.5	1.0	0.7270601
1.5	2.0	0.9503703

Table 8
Effects of f_0 on $f''(0)$ for $Ha = 1.0$ and $K = 1.0$.

λ	f_0	$f''(0)$
0.5	-2.0	-0.4013039
0.5	-1.0	-0.4818197
0.5	0.0	-0.5811208
0.5	1.0	-0.6998513
0.5	2.0	-0.8377182
1.5	-2.0	0.5257285
1.5	-1.0	0.6186625
1.5	0.0	0.7270601
1.5	1.0	0.8511926
1.5	2.0	0.9927172

Tables 9 and 10 depict the effects of the heat generation/absorption parameter ϕ and the chemical reaction parameter γ on the values of $-\theta'(0)$ and $-C'(0)$, respectively. It is seen that irregardless of the value of λ, the value of $-\theta'(0)$ decreases as ϕ increases while the value of $-C'(0)$ increases as γ increases. It should be noted that the value of $-\theta'(0)$ becomes negative for $\phi \geq 0.3$ ($\lambda = 0.5$) and $\phi \geq 1.0$ ($\lambda = 1.5$). This related to the formation of distinctive peaks in the temperature profiles for these values as mentioned before. In addition, it is seen that both of $-\theta'(0)$ and $-C'(0)$ increase as λ increases.

Table 9
Effects of ϕ on $-\theta'(0)$ for $f_0 = 0$, $Ha = 1.0$, $K = 1.0$, and $Pr = 0.023$.

λ	ϕ	$-\theta'(0)$
0.5	-1.0	0.1163904
0.5	0.0	0.0465286
0.5	0.2	0.0184033
0.5	0.3	-0.0029687
0.5	0.4	-0.0375103
1.5	-1.0	0.1319773
1.5	0.0	0.0803958
1.5	0.2	0.0664486
1.5	0.4	0.0501883
1.5	0.6	0.0307590
1.5	0.8	0.0060485
1.5	1.0	-0.0292135

Table 10
Effects of γ on $-C'(0)$ for $f_0 = 0$, $Ha = 1.0$, $K = 1.0$, and $Sc = 0.6$.

λ	γ	$-C'(0)$
0.5	0.0	0.3001323
0.5	1.0	0.6308684
0.5	2.0	0.8390877
0.5	3.0	1.0040110
1.5	0.0	0.4425051
1.5	1.0	0.6908390
1.5	2.0	0.8777776
1.5	3.0	1.0327640

Tables 11 through 14 illustrate the changes in the values of $-\theta'(0)$ and $-C'(0)$ that are brought about by changes in the curvature parameter K and the suction/injection coefficient f_0, respectively. It is observed that, in general, both $-\theta'(0)$ and $-C'(0)$ decrease as K increases while they increase as f_0 increases. However, for the parametric conditions used to produce Table 11, it is seen that for $\lambda = 0.5$, $-\theta'(0)$ decreases as K increases from 0 to 1 while it increases as K increases from 1 to 3. These facts are clearly shown in Tables 11 through 14.

Table 11
Effects of K on $-\theta'(0)$ for $f_0 = 0$, $Ha = 1.0$, $Pr = 0.023$ and $\phi = 0$.

λ	K	$-\theta'(0)$
0.5	0.0	0.0633719
0.5	1.0	0.0465286
0.5	2.0	0.0477679
0.5	3.0	0.0505545
1.5	0.0	0.1027963
1.5	1.0	0.0803958
1.5	2.0	0.0779003
1.5	3.0	0.0769489

Table 12
Effects of K on $-C'(0)$ for $f_0 = 0$, $Ha = 1.0$, $Sc = 0.6$ and $\gamma = 0$.

λ	K	$-C'(0)$
0.5	0.0	0.3630308
0.5	1.0	0.3001323
0.5	2.0	0.2798312
0.5	3.0	0.2702444
1.5	0.0	0.4982547
1.5	1.0	0.4425051
1.5	2.0	0.4203356
1.5	3.0	0.4084820

Table 13
Effects of f_0 on $-\theta'(0)$ for $Ha = 1.0$, $K = 1.0$, $Pr = 0.023$ and $\phi = 0$.

λ	f_0	$-\theta'(0)$
0.5	-2.0	0.0434209
0.5	0.0	0.0465285
0.5	2.0	0.0505405
1.5	-2.0	0.0753895
1.5	0.0	0.0803958
1.5	2.0	0.0859390

Table 14
Effects of f_0 on $-C'(0)$ for $Ha = 1.0$, $K = 1.0$, $Sc = 0.6$ and $\gamma = 0$.

λ	f_0	$-C'(0)$
0.5	-2.0	0.1222565
0.5	0.0	0.3001323
0.5	2.0	0.6007804
1.5	-2.0	0.2229389
1.5	0.0	0.4425051
1.5	2.0	0.7623990

5 Conclusions

The problem of steady, laminar, incompressible, hydromagnetic boundary-layer flow and heat and mass heat transfer over a permeable cylinder moving or stretched with a linear velocity in the presence of heat generation/absorption, chemical reaction, suction/injection effects and uniform transverse magnetic field was formulated. The nonlinear governing partial differential equations were transformed to ordinary differential equations by using useful similarity transformations. The resulting equations were solved numerically by an implicit, iterative finite-difference method. A parametric study of the physical parameters involved in the problem was conducted and the results were illustrated graphically and discussed. Comparisons with previously published work on various special cases of the problem were performed and the results were found to be in excellent agreement. It was found that the skin-friction coefficient was positive for velocity ratios greater than unity and negative for velocity ratios less than unity. When the velocity ratio is less than unity, the skin-friction coefficient increased as either of velocity ratio or the curvature parameter increased while it decreased as the Hartmann number or the suction/injection coefficient increased. On the other hand, when the velocity ratio is greater than unity, the skin-friction coefficient increased as either of the velocity ratio, Hartmann number or the suction/injection coefficient increased while it decreased as the curvature parameter increased. However, in general and irregardless of the velocity ratio, the Nusselt number decreased as either of the heat generation/absorption coefficient or the curvature parameter increased while it increased as the suction/injection coefficient increased. In addition, the Sherwood number was predicted to decrease as the curvature parameter increased while it increased as either of the chemical reaction parameter or the suction/injection coefficient increased. It is hoped that the present results will serve as a stimulus for experimental work dealing with the flow with heat and mass transfer problem discussed in

the present work.

Acknowledgements

The authors would like to thank the anonymous referees for their helpful comments.

References

[1] E.M. Abo-Eldahab, A.M. Salem, MHD Flow and Heat Transfer of Non-Newtonian Power-Law Fluid with Diffusion and Chemical Reaction on a Moving Cylinder, Heat and Mass Transfer 41 (2005) 703-708.
http://dx.doi.org/10.1007/s00231-004-0592-7.

[2] N. Afzal, Heat Transfer from a Stretching Surface, Int. J. Heat Mass Transfer 36 (1993) 1128-1131.
http://dx.doi.org/10.1016/S0017-9310(05)80296-0.

[3] M.E. Ali, Heat transfer characteristics of a continuous stretching surface , Heat and Mass Transfer 29 (1994) 227-234.
http://dx.doi.org/10.1007/BF01539754.

[4] M.E. Ali, On Thermal Boundary Layer on a Power-Law Stretched Surface with Suction or Injection, Int. J. Heat and Fluid Flow 16 (1995) 280-290.
http://dx.doi.org/10.1016/0142-727X(95)00001-7.

[5] M. Amkandi, A. Azzouzi, On a Similarity Solution of MHD Boundary Layer Flow Over a Moving Vertical Cylinder, Differential Equations and Nonlinear Mechanics Volume 2006 (2006) 1-9, Article ID 52765.

[6] W.H.H. Banks, Similarity solutions of the boundary-layer equations for a stretching wall, Journal de Mecanique Theorique et Appliquee European journal of mechanics B Fluids 2 (1983) 375-392.

[7] F.G.Blottner, Finite-Difference Methods of Solution of the Boundary-Layer Equations, AIAA J. 8 (1970) 193-205.
http://dx.doi.org/10.2514/3.5642.

[8] D.E. Bourne, D.G. Elliston, Heat Transfer Through the Axially Symmetric Boundary Layer on a Moving Circular Fibre, Int. J. Heat Mass Transfer 13 (1970) 583-593.
http://dx.doi.org/10.1016/0017-9310(70)90153-5.

[9] A. Chakrabarti, A.S. Gupta, Hydromagnetic Flow and Heat Transfer over a Stretching Sheet, Q. Appl. Math. 37 (1979) 73-78.

[10] A.J. Chamkha, Non-Darcy Hydromagnetic Free Convection from a Cone and a Wedge in Porous Media, Int. Commun. Heat Mass Transfer 23 (1996) 875-887.
http://dx.doi.org/10.1016/0735-1933(96)00070-X.

[11] P. Chandran, N.C. Sacheti, A.K. Singh,Hydromagnetic Flow and Heat Transfer Past a Continuously Moving Porous Boundary, Int. Commun. Heat Mass Transfer 23 (1996) 889-898.
http://dx.doi.org/10.1016/0735-1933(96)00071-1.

[12] C.K. Chen, M. Char, Heat Transfer of a Continuous Stretching Surface with Suction or Blowing , J. Math. Anal. Appl. 135 (1988) 568-580.
http://dx.doi.org/10.1016/0022-247X(88)90172-2.

[13] T.S. Chen, F.A. Strobel, Buoyancy Effects in Boundary Layer Adjacent to a Continuous Moving Horizontal Flat Plate, J. Heat Transfer 102 (1980) 170-172.
http://dx.doi.org/10.1115/1.3244232.

[14] T.C. Chiam, Hydromagnetic Flow over a Surface Stretching with a Power-Law Velocity, Int. J. Engng. Sci. 33 (1995) 429-435.
http://dx.doi.org/10.1016/0020-7225(94)00066-S.

[15] M.H. Cobble, Magnetofluiddynamic Flow with a Pressure Gradient and Fluid Injection, J. Engng. Math. 11 (1977) 249-256.
http://dx.doi.org/10.1007/BF01535969.

[16] L.J. Crane, Flow Past a Stretching Plane, Z. Amgew.Math. Phys. 21 (1970) 645-647.
http://dx.doi.org/10.1007/BF01587695.

[17] L.E. Erickson, L.T.Fan, V.G. Fox, Heat and Mass Transfer on a Moving Continuous Flat Plate with Suction or Injection, Indust. Eng. Chem. 5 (1966) 19-25.

[18] V.G. Fox, L.E. Erickson, L.T. Fan, Methods for Solving the Boundary Layer Equations for Moving Continuous Flat Surfaces with Suction and Injection, AIChE J. 14 (1968) 726-736.
http://dx.doi.org/10.1002/aic.690140510.

[19] P. Ganesan, P. Loganathan, Radiation and Mass Transfer Effects on Flow of an Incompressible Viscous Fluid Past a Moving Vertical Cylinder, Int. J. Heat Mass Transfer 45 (2002) 4281-4288.
http://dx.doi.org/10.1016/S0017-9310(02)00140-0.

[20] P. Ganesan, P. Loganathan, Heat and Mass Flux Effects on a Moving Vertical Cylinder with Chemically Reactive Species Diffusion, Journal of Engineering Physics and Thermophysics 75 (2002) 899-909.
http://dx.doi.org/10.1023/A:1020367102891.

[21] P. Ganesan, P. Loganathan, Magnetic Field Effect on a Moving Vertical Cylinder with Constant Heat Flux, Heat and Mass Transfer 39 (2003) 381-386.

[22] L.G. Grubka, K.M. Bobba, Heat Transfer Characteristics of a Continuous Stretching Surface with Variable Temperature, J. Heat Transfer 107 (1985) 248-250.
http://dx.doi.org/10.1115/1.3247387.

[23] P.S. Gupta, A.S. Gupta, Heat and Mass Transfer on a Stretching Sheet with Suction or Blowing, Canad. J. Chem. Eng. 55 (1977) 744-746.
http://dx.doi.org/10.1002/cjce.5450550619.

[24] A. Ishak, R. Nazar, I. Pop, Magnetohydrodynamic (MHD) Flow and Heat Transfer Due to a Stretching Cylinder, Energy Conversion and Management, 49 (2008) 3265-3269.
http://dx.doi.org/10.1016/j.enconman.2007.11.013.

[25] A. Ishak, R. Nazar, I. Pop, Uniform Suction/Blowing Effect on Flow and Heat Transfer Due to a Stretching Cylinder, Applied Mathematical Modelling 32 (2008) 2059-2066.
http://dx.doi.org/10.1016/j.apm.2007.06.036.

[26] A.M. Jacobi, A Scale Analysis Approach to the Correlation of Continuous Moving Sheet (Backward Boundary Layer) Forced Convective Heat Transfer, J. Heat Transfer 115 (1993) 1058-1061.
http://dx.doi.org/10.1115/1.2911362.

[27] V. Krani, J. Pecho, The Thermal Laminar Boundary Layer on a Continuous Cylinder, Int. J. Heat Mass Transfer 21 (1978) 43-47.
http://dx.doi.org/10.1016/0017-9310(78)90154-0.

[28] K.N. Lakshmisha, S. Venkateswaran, G. Nath, Three Dimensional Unsteady Flow with Heat and Mass Transfer over a Continuous Stretching Surface, J. Heat Transfer 110 (1988) 590-595.
http://dx.doi.org/10.1115/1.3250533.

[29] T.R. Mahapatra, A.S. Gupta, Heat Transfer in Stagnation-Point Flow Towards a Stretching Sheet, Heat and Mass Transfer 38 (2002) 517-521.
http://dx.doi.org/10.1007/s002310100215.

[30] D. Moalem, Steady State Heat Transfer Within Porous Medium with Temperature Dependent Heat Generation, Int. J. Heat Mass Transfer 19 (1976) 529-537.
http://dx.doi.org/10.1016/0017-9310(76)90166-6.

[31] A. Pantokratoras, Laminar Assisting Mixed Convection Heat Transfer from a Vertical Isothermal Cylinder Moving in Water at Low Temperatures, Heat and Mass Transfer 39 (2003) 737-743.
http://dx.doi.org/10.1007/s00231-002-0334-7.

[32] S.R. Pop, T. Grosan, I. Pop, Radiation Effect on the Flow Near the Stagnation Point of a Stretching Sheet, Technische Mechanik 25 (2004) 100-106.

[33] J.W. Rotte, W.J. Beek, Some Models for the Calculation of Heat Transfer Coefficients to a Moving Continuous Cylinder, Chem. Engng. Sci. 24 (1989) 705-716.
http://dx.doi.org/10.1016/0009-2509(69)80063-1.

[34] B.C. Sakiadis, Boundary-Layer Behavior on Continuous Solid Surfaces: I. Boundary-Layer Equations for Two-Dimensional and Axisymmetric Flow, AIChE J. 7 (1961) 26-28.
http://dx.doi.org/10.1002/aic.690070108.

[35] B.C. Sakiadis, Boundary-Layer Behavior on Continuous Solid Surfaces: II. The Boundary-Layer on a Continuous Flat Surface, AIChE J. 7 (1961) 221-225.
http://dx.doi.org/10.1002/aic.690070211.

[36] P.R. Sharma, G. Singh, Effects of Variable Thermal Conductivity and Heat Source/Sink on MHD Flow Near a Stagnation Point on a Linearly Stretching Sheet, Journal of Applied Fluid Mechanics 2 (2009) 13-21.

[37] V.M. Soundalgekar, T.V.R. Murty, Heat Transfer in MHD Flow with Pressure Gradient, Suction and Injection, J. Engng. Math. 14 (1980) 155-159.
http://dx.doi.org/10.1007/BF00037624.

[38] V.M. Soundalgekar, T.V. Ramana Murty, Heat transfer in flow past a continuous moving plate with variable temperature , Heat and Mass Transfer 14 (1980) 91-93.
http://dx.doi.org/10.1007/BF01806474.

[39] E.M. Sparrow, R.D. Cess, Temperature Dependent Heat Sources or Sinks in a Stagnation Point Flow, App. Sci, Res. A10 (1961) 185-197.

[40] H.S. Takhar, A.J. Chamkha, G. Nath, Combined Heat and Mass Transfer Along a Vertical Moving Cylinder with a Free Stream, Heat and Mass Transfer 36 (2000) 237-246.
http://dx.doi.org/10.1007/s002310050391.

[41] F.K. Tsou, E.M. Sparrow, R.J. Goldstein, Flow and Heat Transfer in the Boundary Layer on a Continuous Moving Surface, Int. J. Heat Mass Transfer 10 (1967) 219-235.
http://dx.doi.org/10.1016/0017-9310(67)90100-7.

[42] K. Vajravelu, A. Hadjinicolaou, Convective Heat Transfer in an Electrically Conducting Fluid at a Stretching Surface with Uniform Free Stream, Int. J. Engng Sci. 35 (1997) 1237-1244.
http://dx.doi.org/10.1016/S0020-7225(97)00031-1.

[43] K. Vajravelu, J. Nayfeh, Hydromagnetic Convection at a Cone and a Wedge, Int. Commun. Heat Mass Transfer 19 (1992) 701-710.
http://dx.doi.org/10.1016/0735-1933(92)90052-J.

[44] J. Vleggar, Laminar Boundary-Layer Behavior on Continuous Accelerating Surfaces, Chem. Eng. Sci. 32 (1977) 1517-1525.
http://dx.doi.org/10.1016/0009-2509(77)80249-2.